Published in final edited form as:
Histol Histopathol. 2009 February ; 24(2): 197–207.

Multiple Kallikrein (KLK 5, 7, 8, and 10) Expression in Squamous Cell Carcinoma of the Oral Cavity

Jason R. Pettus[*,1], **Jeffrey J. Johnson**[*,1], **Zonggao Shi**[1], **J. Wade Davis**[2], **Jennifer Koblinski**[3], **Supurna Ghosh**[4], **Yueying Liu**[1], **Matthew J. Ravosa**[1], **Shellaine Frazier**[1], and **M. Sharon Stack**[1,5]

[1]Departments of Pathology & Anatomical Sciences, University of Missouri School of Medicine, Columbia, MO 65212

[2]Department of Health Management & Informatics and Statistics, University of Missouri School of Medicine, Columbia, MO 65212

[3]Pathology, Northwestern University Feinberg School of Medicine, Chicago, IL 60611

[4]Surgery, Northwestern University Feinberg School of Medicine, Chicago, IL 60611

Abstract

Oral squamous cell carcinoma (OSCC) represents 3% of all cancer deaths in the U.S. and is ranked one of the top 10 cancers worldwide. The 5-year survival rate has remained at a low 50% for the past several decades, necessitating discovery of novel biomarkers of aggressive disease and therapeutic targets. As overexpression of urinary type plasminogen activator and receptor (uPA/R) in OSCC is associated with malignant progression and poor outcome, cell lines were generated with either overexpression (SCC25-uPAR+) or silencing (SCC25-uPAR-KD) of uPAR. As SCC25-uPAR+ tumors behaved more aggressively both *in vitro* and *in vivo*, comparative cDNA microarray analysis was used to identify additional genes that may be associated with aggressive tumors. Four members of the human tissue kallikrein family (KLK 5, 7, 8, and 10) were identified and real-time RT-PCR (qPCR) was used to verify and quantify gene expression. qPCR analysis revealed 2.8-, 5.3-, 4.0-, and 3.5-fold increases in gene expression for KLK5, 7, 8, and 10, respectively, in SCC25-uPAR+ *versus* SCC25-uPAR-KD. Immunohistochemical analysis demonstrated strong reactivity for KLKs 5, 7, 8 and 10 in both orthotopic murine tumors and human OSCC tissues. Control experiments show lack of reactivity against KLK3 (prostate specific antigen). These results demonstrate that kallikreins 5, 7, 8, and 10 are abundantly expressed in human OSCC and may be implicated in malignant progression.

Keywords

oral cancer; squamous cell carcinoma; kallikrein

Introduction

Oral cavity cancer results in over 200,000 deaths annually and is one of the top ten most frequently diagnosed cancers worldwide [Parkin et al., 1999]. The most common malignancy

5To whom correspondence should be addressed: M. Sharon Stack, Department of Pathology and Anatomical Science, University of Missouri School of Medicine, M214E Medical Sciences Bldg., 1 Hospital Drive, Columbia, MO 65212, Ph. 573 884 7301, Fax. 573 884 8104, stackm@missouri.edu.
*These two authors contributed equally

of the oral cavity is squamous cell carcinoma (OSCC), with approximately 30,000 new cases detected yearly in the U.S. [Jemal et al., 2006]. The high mortality from OSCC is attributed to regional and distant metastasis and the 5-year survival rate remains at a low 50%. A more detailed understanding of the molecular events that govern OSCC initiation, progression and metastasis may result in identification of novel biomarkers or treatment strategies [Sano and Myers 2000; Macfarlane et al., 1994].

Analyses of human OSCC using cDNA microarray to evaluate genetic changes associated with primary oral tumors, together with immunohistochemical studies, have identified the proteinase urinary type plasminogen activator (uPA, urokinase) as one of 25 genes that comprise an "OSCC gene signature" for molecular classification of oral tumors [Ziober et al., 2006; Nagata et al., 2003]. Together with its receptor (uPAR), tumors exhibiting high uPA/R are more invasive, exhibit enhanced lymph node metastasis [Shi and Stack 2007; Nozake et al., 1998; Lindberg et al., 2006; Yasuda et al., 1997] and more frequent tumor relapse [Hundsdorfer et al., 2005]. We have recently identified a matrix-induced physical interaction between uPA/R and α3β1 integrin that initiates a Src/MEK/ERK-dependent signaling pathway, culminating in enhanced invasive activity *in vitro* [Ghosh et al., 2000; Ghosh et al., 2006] and loss of differentiation status and diffuse infiltrative growth *in vivo* [Ghosh et al; 2009]. To identify additional genes associated with a more aggressive OSCC phenotype, comparative microarray analysis was performed on uPAR overexpressing (SCC25-uPAR+) *versus* uPAR knockdown (SCC25-uPAR-KD) cells. Results identified four members of the tissue kallikrein (KLK) family (KLK 5, 7, 8 and 10) with significantly elevated expression in SCC25-uPAR++ relative to SCC25-uPAR-KD.

The human tissue kallikrein (KLK) family represents fifteen secreted serine proteases encoded by genes co-localized on chromosome 19q13.4. The physiologic roles and natural substrates for most KLKs have not been defined; however expression of multiple KLKs in a single tissue compartment suggests participation in proteolytic cascades [Borgono et al., 2004; Pampalakis and Sotiropoulou 2007; Clements et al., 2004]. Aberrant KLK expression patterns have been reported in many malignancies including those of the breast, prostate, and ovary and have been widely implicated as cancer biomarkers [reviewed in Borgono et al., 2004; Pampalakis and Sotiropoulou 2007; Clements et al., 2004; Paliouras et al., 2004]. Multiple kallikreins have been proposed as both biomarkers and potential therapeutic targets in a number of malignancies. Overexpression of several KLKs may enhance malignant potential both *in vitro* and *in vivo* as KLK activity has been linked to malignant behavior at multiple stages in tumor progression including proliferation, invasion, metastasis and angiogenesis [Borgono et al., 2004; Pampalakis and Sotiropoulou 2007; Clements et al., 2004; Paliouras et al., 2004]. The objective of this study was to validate the cDNA microarray results showing elevated KLK expression in malignant OSCC cells and to investigate the expression of KLKs in oral tumors. Our results indicate that KLKs 5, 7, 8, and 10 are abundantly expressed in human OSCC and may be implicated in malignant progression.

Materials and Methods

Antibodies

Mouse anti-human uPAR clone CD87 (American Diagnostica #3936), 1:20 dilution; rabbit anti-human kallikrein 5 (Abcam #ab28565), 1:20 dilution; rabbit anti-human kallikrein 7 (Abcam #ab28309), 1:20 dilution; rabbit anti-human kallikrein 8 (Abcam #ab28310), 1:20 dilution; rabbit anti-human kallikrein 10 (Abcam #ab28300), 1:20 dilution; rabbit anti-human prostate specific antigen (kallikrein 3) (Abcam #ab9537), 1:2 dilution (supplied at 0.1 mg/ml).

Cell Lines

SCC25 cells were originally derived from OSCC of the human tongue and were the generous gift of Dr. James Rhinewald (Brigham & Women's Hospital, Harvard Institutes of Medicine, Boston, MA). Cells were routinely maintained in DMEM/Ham's F-12 1:1 media containing 10% fetal calf serum and supplemented with 100 units/ml penicillin. Tto generate cells with reduced levels of surface uPAR (SCC25-uPAR-KD), an siRNA knockdown approach was used [Ghosh et al., 2006]. The paired oligonucleotides indicated below were annealed and ligated to BbsI-cut vector (psiRNAhH1neo from Invivogen) and transformed into HB101 competent cells. Target seq2 oligonucleotide 4A (5′-tcccaagccgttacctcgaatgcatttcaagagaatgcattcgaggtaacggctttt-3′) and target seq2 oligo-nucleotide 4B (5′-caaaaaaagccgttacctcgaatgcattctcttgaaatgcattcgaggtaacggctt-3′) DNA was isolated (Qiaprep spin miniprep kit; Qiagen), and the identities of the clones were confirmed by restriction 6 digestion and sequencing with primer OL381 (sequencing primer oligonucleotide OL381, 5′- ccctaactgacacacattcc-3′). Selected clones were then grown in 500-ml cultures, and DNA isolations were done using a nuclease-free DNA isolation kit (Qiagen). SCC25 cells were transfected by electroporation using the human keratinocyte nucleofector kit and device (Amaxa) following the recommended protocol. After 24 h growth under nonselective conditions, the medium was replaced with medium containing 850 μg/ml G418. Loss of uPAR surface expression and purity of clonal cell lines was assessed by fluorescence activated cell sorting (see below).

To generate cells that overexpress uPAR (SCC25-uPAR+), the uPAR sequence was cloned into the expression vector pcDNA 3.1(+) by rtPCR with primer 1: gcgaagcttgggatgggtcacccgccgctg and primer 2: gaattccggtcaggtccagaggagagt. The cDNA was gel-purified using a Qiaquick gel extraction kit (Qiagen), and the cDNA was cut with EcoRI and Hind III and ligated into EcoRI and Hind III – cut vector. The DNA was used to transform HB101 host cells. Cells carrying the pcDNA 3.1-uPAR plasmid were grown in LB medium containing 100 μg/ml ampicillin and plasmid DNA was isolated using a Qiagen DNA Isolation kit. After the uPAR sequence was verified, the DNA was used as template with the following primer sets: PCR Rx 1A: T7 promotor primer + primer 3: cttgtcatcgtcgtccttgtagtcgccccaagaggctgggacgca; and Rx 1B: BGH reverse primer + primer 4: gactacaaggacgacgatgacaagctgcggtgcatgcagtgtaag. The gel-purified cDNA products from Rx's 1A and 1B were used as template for the final PCR Rx 2 using T7 and BGH Rev primers. The resulting uPAR/flag cDNA was cut with EcoRI and Hind III and ligated into EcoRI and Hind III – cut pcDNA 3.1(+) vector. The transformation and DNA purification was carried out as above, and the DNA was used to transfect SCC25 cells. The resulting clonal cell lines were routinely maintained in the medium described above supplemented with G418 and were assessed for expression of uPAR by FACS (see below).

Flow Cytometry

Surface expression of uPAR was determined using flow cytometry [Ghosh et al., 2006], with anti-uPAR (American Diagnostica #3937) at a dilution of 1:100 and fluorescein isothiocyanate conjugated secondary antibody GM488 (Molecular Probes, Eugene, OR) at 1:500. The cells were then washed twice with PBS and resuspended in medium for fluorescence analysis on an Epics XL-MCL flow cytometer (Beckman Coulter, Hialeah, FL). Control experiments contained only the appropriate secondary antibody.

cDNA Microarray

All DNA microarray gene expression studies used human oligonucleotide arrays custom-printed by a dedicated core facility within the Eppley Institute for Research in Cancer and Allied Diseases, University of Nebraska Medical Center (Omaha, NE). Arrays were constructed from a set of 12,140 sense oligonucleotide (60-mers) probes designed for each

human target gene by Compugen Inc. (Rockville, MD) and manufactured by Sigma-Genosys, Inc. (The Woodlands. TX). Individual arrays contain 12,288 spot features, including 12,107 different genes, 28 replications of GAPDH, and negative controls. In brief, approximately 40 μg of experimental and reference RNA samples (i.e., from SCC25-uPAR+ *vs* SCC-25 uPAR-KD) were reverse-transcribed with anchored oligo-dT primer. cDNA was labeled with either Cy3 or Cy5 monofunctional NHS-ester (Amersham Pharmacia). Labeled cDNA in hybridization solution was applied to DNA microarrays and incubated at 42°C for 16-20 h. After hybridization, microarray slides were washed, dried, and scanned immediately with a ScanArray 4000 confocal laser system (Perkin-Elmer). Fluorescent intensities were extracted using the QuantArray software package (Perkin-Elmer).

Statistical Analysis of Microarray Data

Analysis of microarray gene expression data, accumulated from three independent experiments, was performed using the limma package [Smyth 2004], available through the Bioconductor project [Symth 2005] for use with R statistical software [Gentleman et al., 2004]. Data quality was examined by looking for spatial effects across each microarray with image plots of raw log 2 ratios and examining MA-plots of the M-values (log 2 ratios) versus A-values (average log 2 intensities). Both views indicated no large-scale systematic effects indicative of technical problems with the arrays. Background correction was carried out using a normal plus exponential convolution model [Smyth 2005] and print-tip (within-array) loess normalization was used to reduce systematic dye-related bias in the intensity values [Yang et al 2002]. After pre-processing, the analysis of differential gene expression was based on moderated *t*-statistics on the replicated log 2 ratios for each gene. Statistical significance was assessed using an Empirical Bayes approach [Smyth 2004]. Adjustment for multiple comparisons according to the false discovery rate method of Benjamini and Hochberg [Benjamini and Hochberg 1995] was performed, and genes with adjusted *p*-values less than 0.05 were selected as differentially expressed. Log 2 ratios were transformed back to fold change values for interpretation purposes in this report.

Quantitative Real Time PCR (qPCR) Analysis

Selected transcripts identified by cDNA microarray analysis were verified using quantitative real time PCR to validate the mRNA expression level change in SCC25-uPAR+ *vs* SCC25-uPAR-KD cells. Total RNA was extracted with Trizol Reagent (Invitrogen) and reverse transcription was performed with 10 ug of the total RNA from each specimen using SuperScript II reverse transcriptase (Invitrogen) according to the manufacturer's protocol. The cDNA products were then diluted 1:10 and 5 ul of each were used for PCR templates. The following primer sequences were used at final concentrations of 167 nM for each: for **KLK3** (PSA) forward, 5′ – GCATCAGGAACAAAAGCGTGA-3′ and reverse 5′ – CCTGAGGAATCGATTCTTCAG-3′; for **KLK5** forward, 5′ - GCAGGTAGAGACTCCTGCCA-3′ and reverse 5′ - CACAAGGGTAATCTCCCCAG -3′; for **KLK7** forward, 5′ – ACCCTCAGTGCTGGAGAAGA-3′ and reverse 5′ - ACTGGGTCAAAGGTGGTGAA-3′; for **KLK8** forward, 5′ – AAGTGCACCGTCTCAGGC-3′ and reverse 5′ – TCCTCACACTTCTTCTGGGG-3′; for **KLK10** forward, 5′- CTCTGGCGAAGCTGCTG-3′ and reverse 5′ - ATAGGCTTCGGGGTCCAA-3′; for endogenous control gene **phosphoglycerate kinase** (PGK) forward, 5′- GGG CTG CAT- CAC CAT CAT AGG-3′ and reverse 5′- GAG AGC ATC CAC CCC AGG AGG-3′. DNA oligos were custom synthesized (Integrated DNA Technologies). Real-time PCR was performed with SYBR green Master Mix (Aplied Biosystems, Foster City, CA). PCR cycling conditions were 95 C for 13.5 min followed by 40 cycles of 95 C for 15 sec and 60 C for 30 sec. Melt curve cycling consisted of 81 30 sec cycles beginning at 55 C increasing by 0.5 C to 95 C. All reactions were carried out on an iCycleriQ real-time PCR detection system (Bio-Rad Laboratories). Each sample was in triplicate for each

PCR measurement. Melting curves were checked to ensure specificity. Relative quantification of mRNA expression was calculated using the standard curve method with the endogenous housekeeping gene PGK level as normalizer and control sample calibrator.

Orthotopic Sublingual Injections

Murine tongue tumors were generated using six week old female athymic nu/nu mice (Charles River, Wilmington, MA), housed in a specific pathogen-free animal facility and treated according to ACUC protocols. Cells (SCC25-uPAR+ and SCC25-uPAR-KD) were cultured as described above, collected using trypisn, resuspended in PBS and injected into the lateral border of the tongue of anesthetized mice (6.25×10^6 cells in 30 ul sterile PBS) just anterior to the junction of the anterior 2/3 and posterior 1/3 of the tongue [Myers et al. 2002]. At least 8 mice per group were injected, and the experiment was repeated three times. At approximately 9 weeks mice were sacrificed using CO_2, the tongue and cervical lymph nodes were dissected from each mouse, fixed in freshly prepared 4% paraformaldehyde (4°C), paraffin embedded, sectioned (4 μm), and stained with H&E or processed for immunohistochemistry as described below.

Immunohistochemical Analysis

Immunohistochemical analysis was performed on sections of murine tongue tumors or on commercially available microarrayed human OSCC and normal oral tissues (US Biomax OR601 with 50 cases of human OSCC and 10 non-neoplastic oral tissues). Where indicated, serial sections were analyzed to detect expression of multiple antigens expressed in the same tissue area. Paraformaldehyde fixed, paraffin-embedded sections (4 μm) were de-paraffinized with xylene and rehydrated in a series of ethanol washes. Endogenous peroxidase activity was quenched with 3% hydrogen peroxide in methanol for 30 min. Antigen retrieval was enhanced by microwaving in 10mM sodium citrate pH 6.0. Non-specific binding was blocked with 3% normal horse serum in PBS for 30 min. Sections were incubated for 1 hour at room temperature with primary antibody (at dilutions as indicated in Antibody section above) in 1% BSA in PBS. Staining was detected using an avidin-biotin horse radish peroxidase system (Vectastain Universal Elite ABC kit, Cat. # PK-6200, Vector Laboratories, Burlingame, CA, USA), with positive cells staining brown using diaminobenzidine chromogen and hydrogen peroxide substrate (Liquid DAB substrate pack #HK153-5K, BioGenex, San Ramon, CA). Analysis of tissue sections was done by light microscopy by a pathologist (S.F.). Photographs of representative areas of each tumor sample were captured, and immunohistochemical positivity was recorded as a percentage of cells staining with moderate to strong cytoplasmic immunoreactivity per 40× field, not to exceed a cell count of 200 cells per sample. Parametric ANOVA was performed using Systat (San Jose, CA) to compare mean percent staining values between the two groups.

Results

Generation and Analysis of Orthotopic Murine Tumors

Invasive and metastatic OSCC is characterized by enhanced expression of both uPA and its receptor uPAR relative to normal oral mucosa [Ziober et al., 2006; Nagata et al., 2003; Shi & Stack 2007; Nozaki et al., 1998; Lindberg et al., 2006; Yasuda et al., 1997; Hundsdorfer et al., 2005]. Furthermore, recent reports from genome-wide monitoring of genetic changes associated with OSCC primary tumors and lymph node metastases have identified several genes including uPA and the cell-matrix adhesion molecule α3 integrin as predictors of poor disease outcome [Nagata et al., 2003; Al Moustafa et al., 2002]. Our laboratory has recently demonstrated that overexpression of uPAR results in formation of a uPAR/α3β1 integrin complex, resulting in activation of Src/MEK/ERK signaling and activation of target gene transcription [Ghosh et al., 2000; Ghosh et al., 2006], culminating in enhanced invasive activity

in vitro. To evaluate the potential contribution of these molecular interactions to tumor growth and invasion *in vivo*, cells with modified uPAR levels were generated. Relative surface expression levels of uPAR, measured by flow cytometric analysis, were 4.25 +/- 1.21 for SCC25-uPAR-KD and 131.8 +/- 42 for SCC25-uPAR+ (mean fluorescence index). These cells were then injected submucosally into the anterior tongue for *in vivo* analysis. Visual tongue tumors developed by 5-6 weeks and tumors were allowed to progress for 9 weeks. Examination of H&E or cytokeratin-stained sections of tumors formed by SCC25-uPAR-KD cells (Fig. 1A,B,E,F) shows well-circumscribed tumor nests with features characteristic of well-differentiated squamous cell carcinoma, including numerous aggregates of keratin (keratin pearls, **arrowheads**), some dystrophic calcification, low mitotic index and mild nuclear pleomorphism. Most tumor cells showed abundant eosinophilic cytoplasm and a lower nuclear to cytoplasmic ratio than that seen in the uPAR overexpressor group. In contrast, examination of uPAR-overexpressing tumors (SCC25-uPAR+) reveals moderately to poorly differentiated squamous cell carcinoma (Fig. 1C,D,G,H). These tumors are characterized by ill-defined borders and poor circumscription. They are diffusely infiltrative with thin cords of tumor cells dissecting through skeletal muscle (Fig. 1C,D). Clusters of hyperchromatic cells display a high nuclear to cytoplasm ratio and moderate to marked cytologic atypia with only focal keratin production (Fig. 1G,H). No lymph node metastases were detected in either experimental group in the time frame of this study.

Overexpression of uPAR Leads to Altered Kallikrein Expression

Clinical studies of human OSCC show that tumors with high levels of uPA/R are more invasive, exhibit enhanced lymph node metastasis and more frequent tumor relapse [Nozaki et al., 1998; Lindberg et al., 2006; Yasuda et al., 1997; Hundsdorfer et al., 2005]. This is supported by results from orthotopic murine OSCC tumors, showing that overexpression of uPAR leads to less differentiated, more invasive tongue tumors (Fig. 1). These cells were therefore used as a platform for identification of additional genes associated with a more aggressive OSCC phenotype through comparative cDNA microarray analysis using an array containing oligonucleotides corresponding to 12,500 known human genes. Statistical analysis of gene expression in SCC25-uPAR+ *vs* SCC25-uPAR-KD yielded 162 genes that were greater than 2-fold differentially expressed, including four members of the kallikrein (KLK) family of serine proteinases, KLK 5,7, 8, and 10 (Table 1). These candidate genes were validated using real time RT-PCR, confirming significant upregulation (Table 1). Although differential expression of several of KLK genes has previously been associated with prostate, breast and ovarian cancers [15-17], KLK expression in oral SCC has not previously been evaluated.

Based on these results, murine tongue tumors generated from SCC25-uPAR+ or SCC25-uPAR-KD cells were evaluated by immunohistochemical staining of serial sections for expression of KLKs 5, 7, 8 and 10. Staining for KLK3 (also known as prostate specific antigen) was used as a negative control, as upregulation of this KLK family member was not detected by cDNA microarray or qPCR (not shown). Results show a significant increase in percentage of cells staining positive (Table 2) in tumors generated from SCC25-uPAR+ cells (Fig. 2a-h) relative to SCC25-uPAR-KD (Fig. 3a-h). Note that serial sections were used for staining, such that the same tumor is expressing multiple KLKs. No staining for KLK3 was observed in either group (Fig. 2i,j; Fig. 3i,j). KLK expression was also evaluated in serial sections of non-dysplastic human tongue, wherein antibodies to KLK 5,7,8 and 10 stained the lower portion of the stratum superficiale (Fig. 4a-h), while the remainder was predominantly negative. KLK3-specific immunostaining was negative in all zones (Fig. 4i, j). In human oral SCC tumors, immunohistochemical analysis of serial sections demonstrated specific cytoplasmic staining for each KLK in 100% of tumor samples analyzed, with average percentages of positivity: KLK5 - 74%, KLK7 - 66%, KLK8 - 70%, and KLK10 - 76% (Fig. 5a-h). Note that

serial sections were used for staining, such that the same tumor is expressing multiple KLKs. No KLK3 immunoreactivity was detected (Fig. 5i,j).

Discussion

Oral cancers currently represent approximately 3% of all cancer deaths. The five-year survival after diagnosis has remained at a dismal 50% for the past several decades, carrying one of worse prognoses of all cancers. Poor prognosis is directly related to advanced-stage, metastatic disease at the time of diagnosis [Sano & Myers 2007; Macfarlane et al., 1994]. These data highlight the need for new biomarkers of oral SCC incidence, progression, and recurrence. Human tissue KLKs have been shown to be aberrantly expressed in various malignancies, with the most substantial data accumulated by study of hormone-sensitive tumors such as prostate, breast, and ovarian cancer [Borgono et al, 2004; Pampalakis and Sotiropoulou 2007; Clements et al., 2004; Paliouras et al 2004]. While accumulating data support the clinical utility of various KLKs as prognostic biomarkers in these cancers, KLK expression has not previously been reported in oral squamous cell carcinoma. Utilizing both quantitative RT-PCR and immunohistochemical methods, our data indicate that KLKs 5, 7, 8, and 10 are abundantly expressed in oral squamous cell carcinoma, while KLK 3 is not present. Although the current study was not sufficiently statistically powered to identify significant trends between positivity and tumor grade, it is interesting to speculate that acquisition of expression of multiple KLKs may provide a useful clinical parameter for molecular classification of oral SCC lesions.

Multiple KLK expression was identified as upregulated in cells and orthotopic murine oral tumors that also overexpress uPAR. Although the precise mechanism by which uPAR overexpression leads to regulation of KLK expression is unknown, we have previously demonstrated that a matrix-induced complex formation between uPAR and α3β1 integrin leads to sustained integrin signaling via a Src/MEK/ERK pathway, culminating in activation of transcription [Ghosh et al., 2000; Ghosh et al., 2006]. In addition to KLKs, the serine proteinase urinary-type plasminogen activator (uPA, urokinase) and matrix metalloproteinase-9 are also induced by uPAR/α3β1 integrin interaction [Ghosh et al., 2000; Ghosh et al., 2006], suggesting a cellular mechanism by which to enhance pericellular proteolysis.

At present, the potential functional consequences of KLK 5, 7, 8, and 10 expression in OSCC is unknown. A variety of substrates have been described for KLK family enzymes in normal and neoplastic tissues including other KLKs, indicative of participation in zymogen activation cascades [Pampalakis & Sotiropoulou 2007; Clements et al., 2004]. In normal physiologic processes, a tissue KLK cascade involving KLKs 5 and 8 has been shown to regulate semen liquefaction via cleavage of semenogelin I and II [Pampalakis & Sotiropoulou 2007]. In prostate cancer cells, cleavage of insulin-like growth factor binding proteins (IGFBP) 1-5 by KLK5 has been reported, leading to enhanced IGF bioavailability, resulting in aberrant regulation of cell survival and proliferation [Michael et al., 2006]. KLK5 has also been shown to activate proteinase activated receptors (PARs), providing an additional mechanism by which KLK expression may regulate tumor progression [Oikonomopoulou et al., 2005]. Expression of KLKs 5, 7, and 10 have been reported in other tumors as well, including salivary gland [Darling et al., 2006], cervix [Santin et al., 2004] and uterus [Santin et al., 2006], respectively. As in other tumors, analysis of multiple KLK expression may provide additional biomarkers that serve as diagnostic or prognostic indicators for OSCC patients [Paliouras et al., 2004].

Perhaps the best described role for KLKs 5 and 7 is in skin desquamation. Regulation of normal epidermal barrier function is provided by the stratum corneum. Shedding of superficial corneocytes during desquamation is due to proteolytic processing of junctional structures designated corneodesmosomes. KLK5 and KLK7 have been shown to actively participate in this process, through cleavage of corneodesmosin, desmoglein 1 and desmocollin 1 [Borgono

et al, 2004; Caubet et al., 2004; Descargues et al., 2006]. Expression of KLKs 5 and 7 in the stratum superficiale of normal tongue suggests a potentially similar role for these KLKs in the normal oral tongue. Desquamation is regulated by the protease inhibitor lympho-epithelial Kazal-type related inhibitor (LEKTI) encoded by *SPINK5* (serine protease inhibitor Kazal-type 5). Genetic defects in *SPINK5* lead to Netherton syndrome, characterized by severe epidermal fragility, epidermal hyperplasia and a detached stratum corneum [Descargues et al., 2005]. Both KLK5 and KLK7 are inhibited by LEKTI [Deraison et al., 2007; Borgono et al. 2007], and loss of inhibitory function leads to unregulated proteolysis in the outer layers of the epidermis, resulting in defective epidermal barrier function. Interestingly, a recent analysis of genome-wide transcriptome profiles for 53 primary human tongue OSCC tumors relative to 22 normal tongue tissues identified *SPINK5* as a gene that is significantly downregulated in tongue tumors [Ye et al., 2008]. Together with our data showing upregulated KLK expression in tongue OSCC, it is interesting to speculate that uncontrolled KLK activity may contribute to dissolution of tumor cell-cell junctional complexes containing desmoglein 1 and desmocollin 1 and thereby potentiate metastatic dissemination.

Acknowledgments

This research was supported in part by Research Grant RO1 085870 (M.S.S.) from the National Instutitues of Health/ National Cancer Institute. The authors would like to gratefully acknowledge Dr. Hynda Kleinman for her myriad generous contributions to this project.

Literature Cited

Al Moustafa A, Alaoui-Jamali MA, Batist G, Hernandez-Perez M, Serruya C, Alpert L, Black MJ, Sladek R, Foulkes WD. Identification of genes associated with head and neck carcinogenesis by cDNA microarray comparison between matched primary normal epithelial and squamous carcinoma cells. Oncogene 2002;21:2634–40. 298. [PubMed: 11965536]

Benjamini Y, Hochberg Y. Controlling the false discovery rate: a practical and powerful approach to multiple testing. Journal of the Royal Statistical Society Series B 1995;57:289–300.

Borgoño CA, Iacovos PM, Eleftherios PD. Human tissue kallikreins: Physiologic roles and applications in cancer. Mol Cancer Res 2004;2:257–280. [PubMed: 15192120]

Borgono CA, Michael IP, Komatsu N, Jayakumar A, Kapadia R, Clayman GL, Sotiropoulou G, Diamandis EP. A potential role for multiple tissue kallikrein serine proteases in epidermal desquamation. J Biol Chem 2007;282:3640–52. [PubMed: 17158887]

Caubet C, Jonca N, Brattsand M, Guerrin M, Bernard D, Schmidt R, Egelrud T, Simon M, Sere G. Degradation of corneodesmosome proteins by two serine proteases of the kallikrein family, SCTE/ KLK5/hK5 and SCCE/KLK7/hK7. J Invest Dermatol 2004;122:1235–44. [PubMed: 15140227]

Clements JA, Willemsen NM, Myers SA, Dong Y. The tissue kallikrein family of serine proteases: functional roles in human disease and potential as clinical biomarkers. Crit Rev Clin Lab Sci 2004;41:265–312. [PubMed: 15307634]

Darling MR, Tsai S, Jackson-Boeters L, Daley TD, Diamandis EP. Human kallikrein 3 and human kallikrein 5 expression in salivary gland tumors. Int J of Biological Markers 2006;21:201–5.

Deraison C, Bonnart C, Lopez F, Besson C, Robinson R, Jayakumar A, Wagberg F, Brattsand M, Hachem JP, Leonardsson G, Hovnanian A. LEKTI fragments specifically inhibit KLK5, KLK7 and KLK14 and control desquamation through a pH dependent interaction. Mol Biol Cell 2007;18:3607–19. [PubMed: 17596512]

Descargues P, Deraison C, Prost C, Fraitag S, Mazereeuw-Hautier J, D'Alessio M, Ishida-Yamamamoto A, Bodemer C, Zambruno G, Hovnanian A. Corneodesmosomal cadherins are preferential targets of stratum corneum trypsin- and chymotrypsin-hyeractivity in Netherton syndrome. J Invest Dermatol 2006;126:1622–32. [PubMed: 16628198]

Descargues P, Deraison C, Bonnart C, Kreft M, Kishibe M, Ishida-Yamamoto A, Elias P, Barrandon Y, Zambruno G, Sonnenberg A, Hovnanian A. Spink5-deficient mice mimic Netherton syndrome

through degradation of desmoglein 1 by epidermal protease hyperactivity. Nature Genetics 2005;37:56–63. [PubMed: 15619623]

Gentleman RC, Carey VJ, Bates DM, et al. Bioconductor: open software development for computational biology and bioinformatics. Genome Biol 2004;5:R80. [PubMed: 15461798]

Ghosh S, Brown R, Jones JCR, Ellerbroek SM, Stack MS. Urinary-type plasminogen activator (uPA) expression and uPA receptor localization are regulated by α3β1 integrin in oral keratinocytes. J Biol Chem 2000;275:23869–76. [PubMed: 10791952]

Ghosh S, Johnson JJ, Sen R, Mukhopadhyay S, Liu Y, Zhang F, Wei Y, Chapman HA, Stack MS. Functional relevance of urinary-type plasminogen activator receptor-α3β1 integrin association in proteinase regulatory pathways. J Biol Chem 2006;281:13021–29. [PubMed: 16510444]

Ghosh, S.; Koblinski, J.; Johnson, J.; Liu, Y.; Frazier, S.; Ericcson, A.; Shi, Z.; Ravosa, MJ.; Crawford, S.; Stack, MS. Urinary-Type Plasminogen Activator Receptor (uPA/R)/α3β1 Integrin Signaling and Oral Tumor Progression (submitted).

Jemal A, Siegel R, Ward E, Murray T, Xu J, Smigal C, et al. Cancer statistics, 2006. CA: A Cancer Journal for Clinicians 2006;56:106–130. [PubMed: 16514137]

Hundsdorfer B, Zeilhofer HF, Bock KP, Dettmar P, Schmitt M, Kolk A, Pautke C, Horch HH. Tumor associated urokinase type plasminogen activator and its inhibitor PAI1 in normal and neoplastic tissues of patients with squamous cell cancer of the oral cavity – clinical relevance and prognostic value. J Craniomaxillofac Surg 2005;33:191–6. [PubMed: 15878520]

Lindberg P, Larsson A, Nielsen BS. Expression of plasminogen activator inhibitor-1, urokinase receptor and laminin gamma 2 chain is an early coordinated event in incipient oral squamous cell carcinoma. Int J Cancer 2006;118:2948–2956. [PubMed: 16395714]

Macfarlane, Gl; Boyle, P.; Evstifeeva, TV.; Robertson, C.; Scully, C. Rising trends of oral cancer mortality among males worldwide: the return of an old public health problem. Cancer Causes Control 1994;5:2259–265.

Michael IP, Pampalkis G, Miklajczyk SD, Malm J, Sotiropoulou G, Diamandis EP. Human tissue kallikrein 5 is a member of a proteolytic cascasde pathway involved in seminal clot liquefaction and potentially in prostate cancer progression. J Biol Chem 2006;281:12743–50. [PubMed: 16517595]

Myers JN, Holsinger FC, Jasser SA, Bekele BN, Fidler IJ. An orthotopic nude mouse model of oral tongue squamous cell carcinoma. Clinical Cancer Research 2002;8:293. [PubMed: 11801572]

Nagata M, Fujita H, Ida H, Hoshina H, Inoue T, Seki Y, Ohnishi M, Ohyama T, Shingaki S, Kaji M, et al. Identificaiton of potential biomarkers of lymph node metastasis in oral squamous cell carcinoma by cDNA microarray analysis. Int J Cancer 2003;106:683–689. [PubMed: 12866027]

Nozaki S, Endo Y, Kawashiri S, Nakagawa K, Yamamoto E, Yonemura Y, Sasaki T. Immunohistochemical localization of a urokinase-type plasminogen activator system in squamous cell carcinoma of the oral cavity: association with mode of invasion and lymph node metastasis. Oral Oncol 1998;34:58–62. [PubMed: 9659521]

Oikonomopoulou K, Hansen KK, Saifedine M, Tea I, Blabber M, Blabber SI, Scarisbrick I, Andrade-Gordon P, Cottrell GS, Bunnett NW, Diamandis EP, Hollenberg MD. Protease activated receptors: targets for kallikrein signaling. J Biol Chem 2005;281:32095–112. [PubMed: 16885167]

Paliouras M, Borgono C, Diamandis EP. Human tissue kallikreins: the cancer biomarker family. Cancer Letters 2004;249:61–79. [PubMed: 17275179]

Pampalakis G, Sotiropoulou G. Tissue kallikrein proteolytic cascade pathways in normal physiology and cancer. Biochimica et Biophysic Acta 2007;1776:22–31.

Parkin DM, Pisani P, Ferlay J. Global cancer statistics. CA: A Cancer Journal for Clinicians 1999:33–64. [PubMed: 10200776]

Sano D, Myers JN. Metastasis of squamous cell carcinoma of the oral tongue. Cancer Metastasis Rev 2007;26:645–62. [PubMed: 17768600]

Santin AD, Cane S, Bellone S, Bignotti E, Palmieri M, De Las Casas LE, Roman JJ, Anfossi S, O'Brien T, Pecorelli S. The serine protease stratum corneum chymotryptic enzyme (kallikrein 7) is highly overexpressed in cervical cancer cells. Gyn Oncol 2004;94:283–88.

Santin AD, Diamandis EP, Bellone S, Marizzoni M, Bandiera E, Palmieri M, Papasakelariou C, Katsaros D, Burnett A, Pecorelli S. Overexpression of kallikrein 10 (hK10) in uterine serous papillary carcinomas. Am J Ob Gyn 2006;194:1296–302.

Shi Z, Stack MS. Urinary-type plasminogen activator (uPA) and its receptor (uPAR) in squamous cell carcinoma of the oral cavity. Biochem J 2007;407:153–9. [PubMed: 17880283]

Smyth, GK. Linear models and empirical Bayes methods for assessing differential expression in microarray experiments. Statistical Applications in Genetics and Molecular Biology. 2004. Article 3 http://www.bepress.com/sagmb/vol3/iss1/art3

Smyth, GK. Limma: linear models for microarray data. In: Gentleman, R.; Carey, V.; Dudoit, S.; Irizarry, R.; Huber, W., editors. Bioinformatics and Computational Biology Solutions using R and Bioconductor. Springer; New York: 2005. p. 397-20.

Yang YH, Dudoit S, Luu P, Lin DM, Peng V, Ngai J, Speed TP. Normalization for cDNA microarray data: a robust composite method addressing single and multiple slide systematic variation. Nucleic Acids Research 2002;30(4):e15. [PubMed: 11842121]

Yasuda T, Sakata Y, Kitamura K, Morita M, Ishida T. Localization of plasminogen activators and their inhibitor in squamous cell carcinomas of the head and neck. Head Neck 1997;19:611–6. [PubMed: 9323150]

Ye H, Yu T, Temam S, Ziober BL, Wang J, Schwartz JL, Mao L, Wong DT, Zhou X. Transcriptomic dissection of tongue squamous cell carcinoma. BMC Genomics 2008;6:69. [PubMed: 18254958]

Ziober AF, Patel KR, Alawi F, Gimotty Ph, Weber RS, Feldman MM, Chalian AA, Weinstein GS, Hunt J, Ziober BL. Identification of a gene signature for rapid screening of oral squamous cell carcinoma. Clin Can Res 2006;12:5960–71.

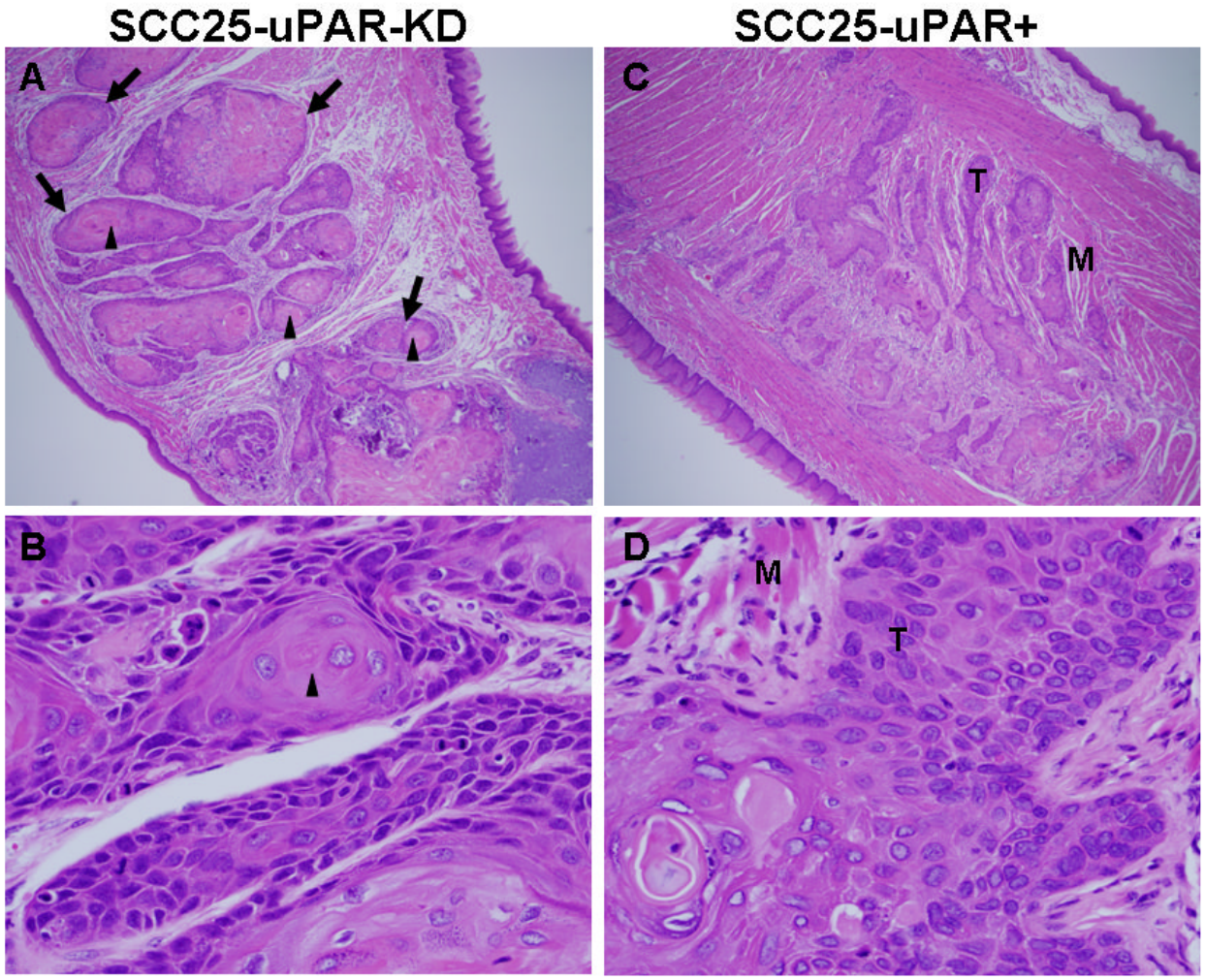

Fig 1A-D

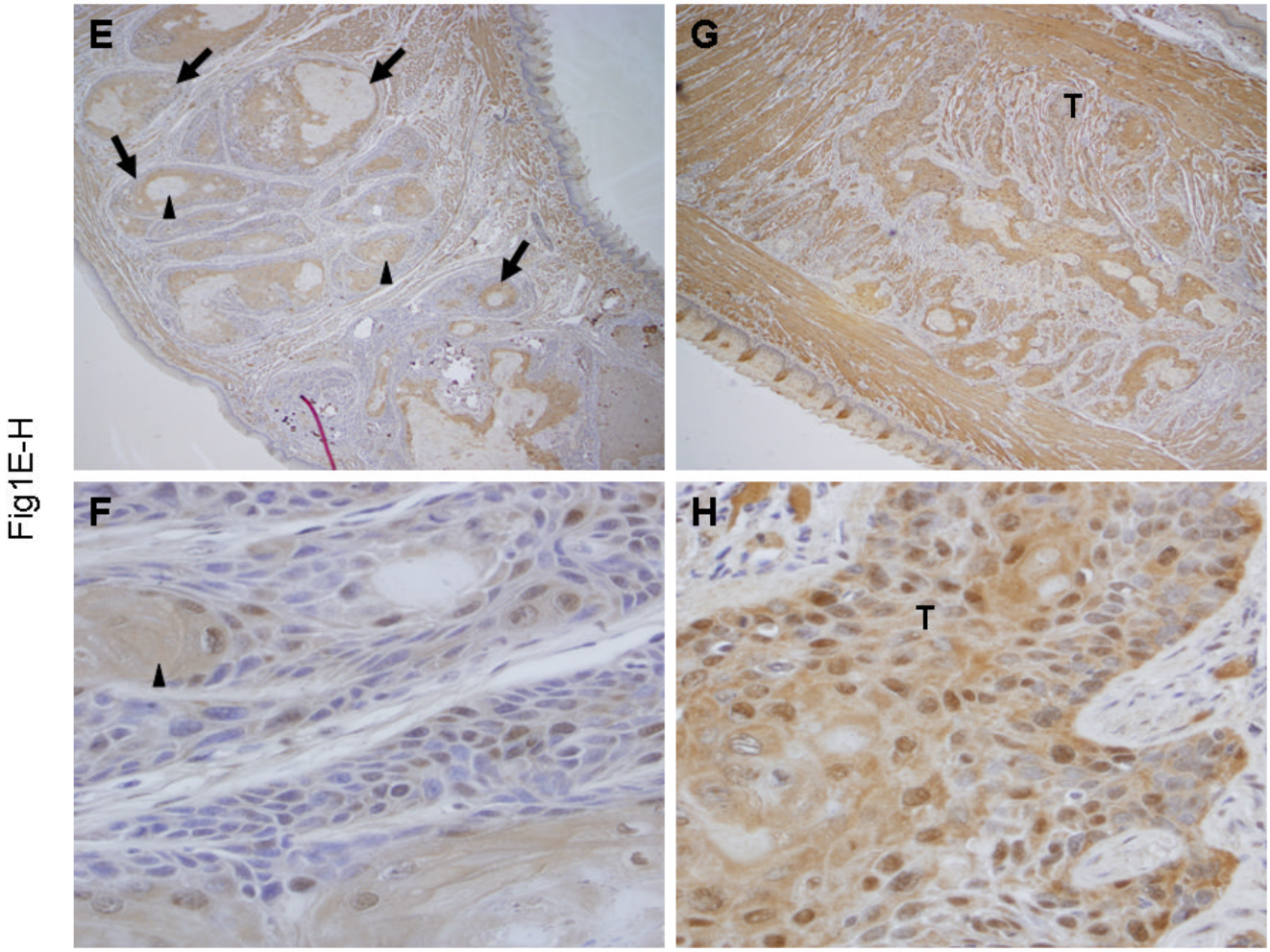

Fig. 1. Histology of SCC25-uPAR-KD and SCC25-uPAR+ murine oral tongue tumors

Tumors generated from pooled clones of SCC25-uPAR-KD and SCC25-uPAR+ cells were (A-D) stained with H&E (E-H) or immunostained with anti-cytokeratin AE1/AE3 (M3515, 1:25 dilution) followed by a biotinylated secondary antibody and detection of avidin-biotin with DAB chromagen and substrate as in Experimental Procedures. Panels A, C, E, G are 40× magnification; panels B,D, F, H are 400×. (T) – designates areas of tumor cells; (M) designates host tongue muscle; (arrowheads) – focal keratinization ('keratin pearls' are highlighted); (arrows) – example of well-circumscribed tumor nests.

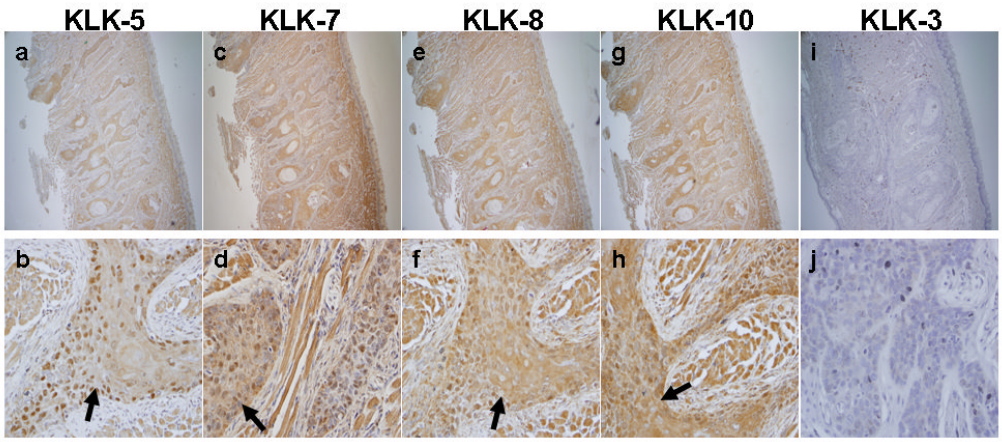

Fig. 2. Immunohistochemical analysis of multiple KLK expression in SCC25-uPAR+ murine oral tongue tumors

Serial sections of tumors generated from pooled clones of SCC25-uPAR+ cells were immunostained with antibodies against (a,b) KLK5, (c,d) KLK7, (e,f) KLK8, (g,h) KLK10, or (i,j) KLK3 at the dilutions provided in Experimental Procedures followed by a biotinylated secondary antibody and detection of avidin-biotin with DAB chromagen and substrate. Panels a,c,e,g,I − 40× magnification; panels b,d,f,g,j − 400× magnification. Arrows denote tumor cell nests staining positive for the respective KLK. Identical immunoreactivity in serial sections stained for KLK5, KLK7, KLK8 and KLK10 indicates expression of multiple KLKs by the same tumor cell nest.

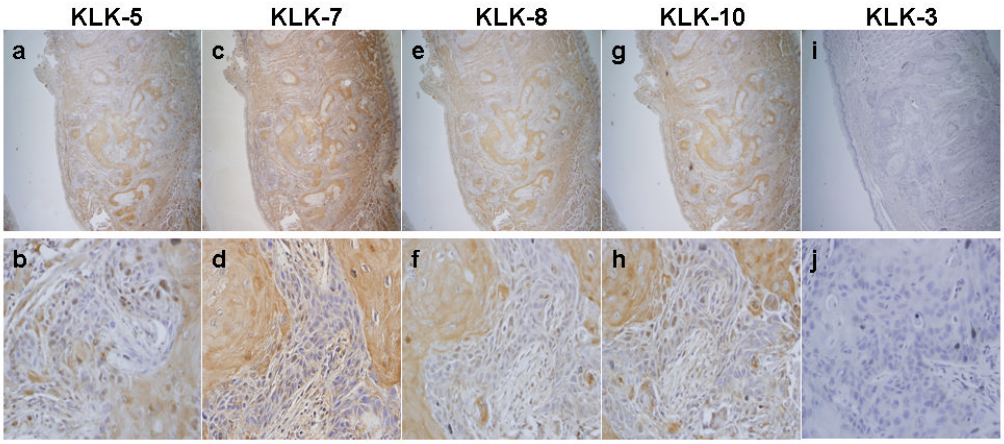

Fig. 3. Immunohistochemical analysis of multiple KLK expression in SCC25-uPAR-KD murine oral tongue tumors

Serial sections of tumors generated from pooled clones of SCC25-uPAR-KD cells were immunostained with antibodies against (a,b) KLK5, (c,d) KLK7, (e,f) KLK8, (g,h) KLK10, or (i,j) KLK3 at the dilutions provided in Experimental Procedures followed by a biotinylated secondary antibody and detection of avidin-biotin with DAB chromagen and substrate. Panels a, c, e, g, i − 40× magnification; panels b, d, f, g, j − 400× magnification. Identical immunoreactivity in serial sections stained for KLK5, KLK7, KLK8 and KLK10 indicates expression of multiple KLKs by the same tumor cell nest, although staining intensity is significantly reduced relative to uPAR+ tumors (Fig. 2).

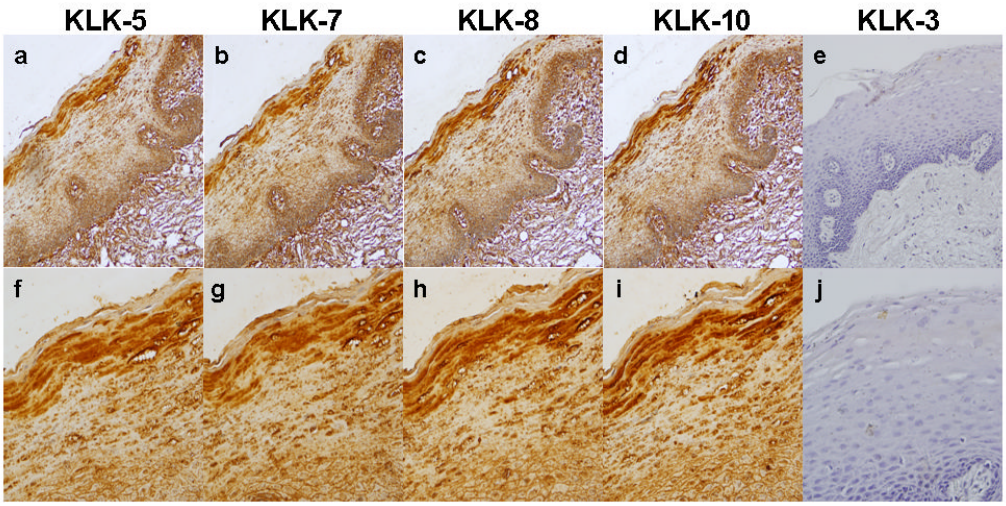

Fig. 4. Immunohistochemical analysis of multiple KLK expression in normal human oral mucosa

Serial sections of normal tongue were immunostained with antibodies against (a,b) KLK5, (c,d) KLK7, (e,f) KLK8, (g,h) KLK10, or (i,j) KLK3 at the dilutions provided in Experimental Procedures followed by a biotinylated secondary antibody and detection of avidin-biotin with DAB chromagen and substrate. Panels a, c, e, g, i − 40× magnification. Panels b, d, f, g, j − 400× magnification of the lower portion of the stratum superficiale.

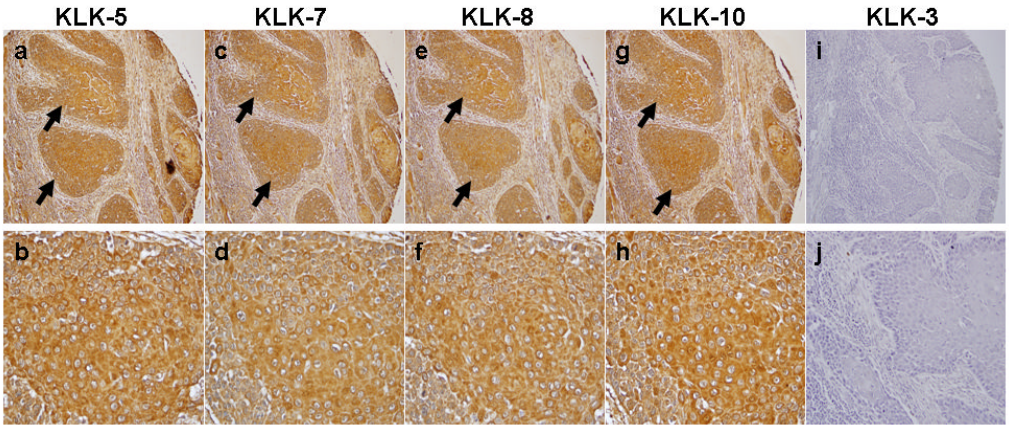

Fig. 5. Immunohistochemical analysis of multiple KLK expression in human oral tongue tumors

Sections of human OSCC of the oral tongue were immunostained with antibodies against (a,b) KLK5, (c,d) KLK7, (e,f) KLK8, (g,h) KLK10, or (i,j) KLK3 at the dilutions provided in Experimental Procedures followed by a biotinylated secondary antibody and detection of avidin-biotin with DAB chromagen and substrate. Panels a,c,e,g,I − 40× magnification; panels b,d,f,g,j − 400× magnification. Arrows denote tumor cell nests staining positive for the respective KLK. Identical immunoreactivity in serial sections (a-h) stained for KLK5, KLK7, KLK8 and KLK10 indicates expression of multiple KLKs by the same tumor cell nest. KLK3 immunoreactivity is not observed.

Table 1
cDNA Microarray and qPCR Analysis of KLK Expression

cDNA Microarray	Mean Fold Δ (SCC25-uPAR+ / SCC25-uPAR-KD)	Mean Expression	*p*	
			Raw	Adjusted
KLK-5	6.06	1730	0.00047	.040
KLK-7	3.97	513	0.00012	.018
KLK-8	5.53	924	0.00012	.018
KLK-10	5.38	568	0.00017	.020
qPCR	**SCC25-uPAR+**	**SCC25-uPAR-KD**	**RQ**	
KLK-5	0.272	0.096	2.8×	
KLK-7	0.078	0.015	5.3×	
KLK-8	0.186	0.046	4.0×	
KLK-10	0.034	0.01	3.5×	

cDNA microarray - Mean fold change of SCC25-uPAR+ *vs* SCC25-uPAR-KD based on results for cDNA microarray experiments. Average intensity of the two channels indicates good signal quality and that the results are not artifacts due to comparison of weak signals. P-values before and after adjustment for multiple testing reflect the strong degree of evidence that the genes are differentially expressed between the two groups.

qPCR - Real time RT-PCR relative quantification (RQ) of each kallikrein in SCC25-uPAR+ *vs* SCC25-uPAR-KD cells. The center columns represent qPCR data based on experimental Ct values that have been standardized to PGK-1 housekeeping gene via the standard curve method.

Table 2
Analysis of KLK 5, 7, 8, and 10 Expression in Murine OSCC

KLK	% positive SCC25-uPAR+	% positive SCC25-uPAR-KD	p value
KLK-5	73.3 +/- 6.3	33.3 +/- 16.2	<.001
KLK-7	72.0 +/- 8.9	29.5 +/- 9.80	<.001
KLK-8	81.3 +/- 7.5	41.9 +/- 24.3	<.001
KLK-10	87.6 +/- 4.9	33.9 +/- 18.6	<.001

Tumors were generated from SCC25-uPAR+ or SCC25-uPAR-KD cells and immunostained for KLK 5, 7, 8, or 10 as described in Materials and Methods. Immunohistochemical positivity was recorded as a percentage of cells staining with moderate to strong immunoreactivity per 40× field. A minimum of 10 fields was counted per condition. Shown are mean and standard deviation. Parametric ANOVA was performed (Systat, San Jose, CA) to compare the mean % staining values between the two groups.